PROCEEDINGS

SPIE—The International Society for Optical Engineering

# Advanced Signal-Processing Algorithms, Architectures, and Implementations

**Franklin T. Luk**
*Chair/Editor*

**10–12 July 1990**
**San Diego, California**

SPIE P PROCEEDINGS SERIES

**Volume 1348**

S.Oh, R.J. Marks II, L.E. Atlas and J.W. Pitton,
"Kernel synthesis for generalized time-frequency distributions using the method of projection onto convex sets",
SPIE Proceedings 1348, Advanced Signal Processing Algorithms, Architectures, and Implementation,
F.T. Luk, Editor, pp.197-207, San Diego, July 10-12, 1990.

# Kernel Synthesis for Generalized Time-Frequency Distributions Using the Method of Projections Onto Convex Sets

Seho Oh, R.J. Marks II, L.E. Atlas, J.W. Pitton
Interactive System Design Laboratory
Department of Electrical Engineering, FT-10
University of Washington
Seattle, WA 98195, U.S.A.

## Abstract

The kernel in Cohen's generalized time-frequency representation (GTFR) requires is chosen in accordance to certain desired performance attributes. Properties of the kernel are typically expressed as constraints. We establish that many commonly used constraints are convex in the sense that all allowable kernels satisfying a given constraint form a convex set. Thus, for a given set of constraints, the kernel can be designed by alternately projecting among these sets. If there exists a nonempty intersection among the constraint sets, then the theory of *projection onto convex sets* (POCS) guarantees convergence to a point in the intersection. If the constraints can be partitioned into two sets, each with a nonempty intersection, then POCS guarantees convergence to a kernel that satisfies the inconsistent constraints with minimum mean square error.

## 1 Introduction

The generalized time-frequency representation (GTFR) of a temporal signal, $x(t)$, can be written as [5, 6]

$$C(t;u) = \int_{-\infty}^{\infty}\int_{-\infty}^{\infty} \hat{\phi}(t-\xi;\tau) \times x(\xi+\frac{\tau}{2})x^*(\xi-\frac{\tau}{2})e^{-j2\pi u\tau}d\xi d\tau \quad (1)$$

where $\hat{\phi}(t;\tau)$ is the kernel of the GTFR and $u$ is the frequency variable. The choice of the kernel dictates the performance of the GTFR. Typically, constraints are placed on the kernel in order to enhance various aspects of the GTFR [3, 5, 6, 7, 8, 9, 20].

In order to facilitate discussion, we define the following Fourier transforms on the kernel.

$$\phi(f,\tau) = \int_{t=-\infty}^{\infty} \hat{\phi}(t,\tau)e^{-j2\pi ft}dt, \quad (2)$$

$$\hat{\Phi}(t,u) = \int_{\tau=-\infty}^{\infty} \hat{\phi}(t,\tau)e^{-j2\pi u\tau}d\tau, \quad (3)$$

| | $t$ | $f$ |
|---|---|---|
| $\tau$ | $\hat{\phi}(t,\tau) \rightarrow$ | $\phi(f,\tau)$ |
| | $\downarrow$ | $\downarrow$ |
| $u$ | $\hat{\Phi}(t,u) \rightarrow$ | $\Phi(f,u)$ |

Table 1: The kernel for Cohen's GTFR expressed in various Fourier transform domains. Each arrow corresponds to a one-dimensional Fourier transform.

and

$$\Phi(f,u) = \int_{-\infty}^{\infty}\int_{-\infty}^{\infty} \hat{\phi}(t,\tau) \times e^{-j2\pi(u\tau+ft)}dtd\tau, \quad (4)$$

The various forms of the kernel are summarized in Table 1.

## 2 Kernel Constraints

Using the kernels summarized in Table 1, we can straightforwardly state some of the commonly used constraints imposed on the GTFR and their corresponding interpretation as kernel constraints.

1. **Time Resolution Constraint.**

   The requirement that the input on the interval $-T \leq t-\xi \leq T$ contribute to the GTFR only on the same interval can be cast as a *cone constraint*. This requires that $\hat{\phi}(t;\tau)$ be identically zero outside of the cone shown in Fig. 1. In other words,

   $$\hat{\phi}(t;\tau) = \hat{\phi}(t;\tau)\Pi(\frac{t}{\tau})\Pi(\frac{\tau}{2T}) \quad (5)$$

   where the rectangle function, $\Pi(t)$, is one for $\mid t \mid \leq \frac{1}{2}$ and is zero otherwise.

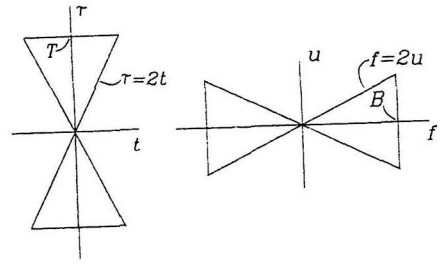


Figure 1: The cone and bow tie constraints. On the $(t,\tau)$ plane shown on the left, the kernel $\hat{\phi}(t;\tau)$ is zero outside the cone shown if it is to obey the time resolution constraint. The set of all such functions obeying this constraint is convex. The dual frequency resolution constraint requires $\Phi(f;u)$ to be zero outside of the bow tie shown on the right. The set of all functions obeying this constraint is also convex.

2. **Interference Suppression Constraint.**

   The magnitude of the interference at frequency $f$ between two tones at frequencies $f_1$ and $f_2$ is zero when [14]

   $$\Phi(f_1-f_2; f-\frac{f_1+f_2}{2}) = 0 \quad (6)$$

   With attention focused on the $u$ variable of $\Phi(f;u)$, this constraint is met if

   $$\Phi(f,u) = \Theta(u)\delta(f) \quad (7)$$

   where $\Theta(u)$ is an arbitrary one dimensional function and $\delta(f)$ is the Dirac delta. This is equivalent to requiring that

   $$\hat{\phi}(t,\tau) = \theta(\tau) \quad (8)$$

   A relaxed interference constraint is

   $$\Phi(f,u) = \Phi(f,u)\Pi(\frac{f}{2\Delta}) \quad (9)$$

where $\Delta$ is an interference bandwidth interval.

3. **Frequency Resolution Constraint.**

The GTFR in Equation 1 can also be written as

$$C(t;u) = \int_{-\infty}^{\infty}\int_{-\infty}^{\infty} \Phi(f;u-\nu) \times X(\nu+\frac{f}{2})X^*(\nu-\frac{f}{2}) \times e^{j2\pi ft}d\nu df \quad (10)$$

Comparing with Equation 1 immediately suggests a frequency resolution constraint that is the dual of the cone constraint in Equation 5.

$$\Phi(f;u) = \Phi(f;u)\Pi(\frac{f}{u})\Pi(\frac{f}{2B}) \quad (11)$$

where $B$ is the frequency dual of $T$.

4. **Power Spectral Density Marginal Constraint.**

Define the power spectral density of a signal $x(t)$ by

$$P(u) = \int_{-\infty}^{\infty} R(\tau)e^{-j2\pi u\tau}d\tau \quad (12)$$

where the autocorrelation of the signal is

$$R(\tau) = \int_{-\infty}^{\infty} x(\xi+\frac{\tau}{2})x^*(\xi-\frac{\tau}{2})d\xi \quad (13)$$

A desirable property of a GTFR is the power spectral marginal constraint

$$P(u) = \int_{-\infty}^{\infty} C(t,u)dt \quad (14)$$

This is clearly achieved if

$$\int_{-\infty}^{\infty} \hat{\phi}(t,\tau)dt = 1 \quad (15)$$

This is equivalent to requiring that

$$\phi(0,\tau) = 1 \quad (16)$$

5. **Power Marginal Constraint.**

Similar to the previous power spectral density marginal, we desire to have an instantaneous power marginal.

$$|\, x(t)\,|^2 = \int_{-\infty}^{\infty} C(t,u)du \quad (17)$$

This is achieved when

$$\phi(f,0) = 1 \quad (18)$$

6. **Realness Constraint.** A sufficient condition for $C(t,u)$ to be real is that the kernel be conjugately symmetric.

$$\phi(f,\tau) = \phi^*(-f,-\tau) \quad (19)$$

This is equivalent to requiring that $\hat{\Phi}(t,u)$ is real.

$$\Re\hat{\Phi}(t,u) = \hat{\Phi}(t,u) \quad (20)$$

where $\Re$ denotes *the real part of.*

7. **Time Symmetry Constraint.**

At a given point temporal point, past and future time are symmetrically treated if

$$\phi(f,\tau) = \phi^*(f,-\tau) \quad (21)$$

Note that, assuming differentiablity, that it follows that

$$\frac{\partial\phi(f,\tau)}{\partial\tau}\,|_{\tau=0} = 0 \quad (22)$$

8. **Frequency Symmetry Constraint.**

   Similarly, for frequency symmetry, we impose the constraint

$$\phi(f,\tau) = \phi^*(-f,\tau). \qquad (23)$$

   Again, assuming differetiability, this requires that

$$\frac{\partial\phi(f,\tau)}{\partial f}\,|_{f=0} \;= 0 \qquad (24)$$

   Note that imposition of any two of the previous three constraints imposes the third.

9. **Non-negativity Constraint.**

   We may wish to require that the kernel is positive in the sense that

$$\hat{\phi}(f,\tau) = \Re\hat{\phi}(-f,\tau)\mu[\Re\hat{\phi}(-f,\tau)] \qquad (25)$$

   where $\mu(\cdot)$ is the unit step. In other words, the real part of $\hat{\phi}(f,\tau)$ is non-negative.

# 3 POCS

All of the constraints in the previous section are convex in the sense that, if the kernels $\phi_1$ and $\phi_2$ satisfy a particular constraint, then, for any $\alpha$ in the interval $0 \leq \alpha \leq 1$, the kernel $\alpha\phi_1 + (1-\alpha)\phi_2$ satisfies the same constraint. The convexity of the constraints allows use of the powerful synthesis procedure of *projection onto convex sets* (POCS). POCS was initially introduced by Youla & Webb [18] and Sezan & Stark [15] and has been applied to such topics as sampling theory [17], fuzzy set theory [4] and artificial neural networks [11, 12]. The synthesis of GTFR kernels using POCS closely parallels the synthesis of windows proposed by Goldburg and Marks [10]. A superb overview of POCS with other applications is in the book by Stark [16].

We now present an abbreviated introduction to POCS.

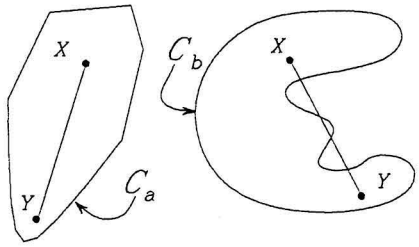


Figure 2: The set $C_a$ on the left is convex. All line segments with endpoints $X$ and $Y$ within the set are totally subsumed within the set. The set $C_b$ on the right is clearly not convex as illustrated by the counter example shown.

## 3.1 Convex Sets

Let $\mathcal{C}$ denote a set of functions. The set $\mathcal{C}$ is said to be convex if, for every $X \in \mathcal{C}$ and $Y \in \mathcal{C}$,

$$\alpha X + (1-\alpha)Y \in \mathcal{C} \;; 0 \leq \alpha \leq 1.$$

Geometrically, this is interpreted as shown in Figure 2. A set is convex if, for every two points chosen within the set, all of the points in the line segment connecting the two points are also in the set. The set on the left in Figure 2 is convex. Geometrical shapes corresponding to convex sets include balls, line segments, planes, boxes and quadrants. The set shown on the right in Figure 2 is clearly not convex.

## 3.2 Convex Set Projections

The *projection* of an arbitrary function $Z$, onto a (compact) convex set $\mathcal{C}$ is the unique function in $\mathcal{C}$ that is closest to $Z$ in the mean square sense. This is geometrically illustrated in Figure 3. Denote the projection operator by $\mathcal{P}_{\mathcal{C}}Z$. Note that, if $Z \in \mathcal{C}$, then $\mathcal{P}_{\mathcal{C}}Z = Z$. In other

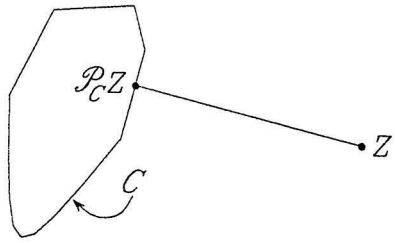


Figure 3: As illustrated here, the projection of a function $Z$ onto the convex set $C$ is that unique point in $C$ that is closest to $Z$ in the mean square sense. The result of the projection is the point $\mathcal{P}_C Z$.

words, if a function is already within the set, then the projection is an identity operation. It follows that ${\mathcal{P}_C}^2 = \mathcal{P}_C$.

We illustrate with sample projection operators from the convex constraints of the Cohen kernel in the previous section. A more extensive list of projection operators can be found in Youla & Webb's paper [18] and in Stark's book [16]. In the examples here, we will use the form of the kernel in Table 1 that most easily explains the projection. Any of the four choices of domains can be accessed from any other by appropriate Fourier transformation. Inherent in the projection notation is the assumption that the kernel is in the proper domain.

1. **Time & Frequency Resolution Projections.**

   For the time resolution Constraint 1, the signal outside of the cone on the $(t,\tau)$ plane is simply set to zero.

$$\mathcal{P}_{C1}\hat{\phi}(t,\tau) = \hat{\phi}(t,\tau) \times \Pi(\frac{t}{\tau})\Pi(\frac{\tau}{2T}) \qquad (26)$$

   Similarly, for frequency resolution constraint 3, the area outside of the bow tie on the $(f,u)$ plane is set to zero.

$$\mathcal{P}_{C3}\Phi(f,u) = \Phi(f;u) \times \Pi(\frac{f}{u})\Pi(\frac{f}{2B}) \qquad (27)$$

2. **Realness & Symmetry Constraint.**

   Realness Constraint 6 can be imposed by the projection operator

$$\mathcal{P}_{C6}\hat{\Phi}(t,u) = \Re\hat{\Phi}(t,u) \qquad (28)$$

   or, equivalently, in the $(f,\tau)$ plane,

$$\mathcal{P}_{C6}\phi(f,\tau) = \frac{1}{2}[\phi(f,\tau) + \phi^*(-f,-\tau)]. \qquad (29)$$

   Similarly, for the symmetry constraints in Equations 21 and 23, the respective projection operators can be written as

$$\mathcal{P}_{C7}\phi(f,\tau) = \frac{1}{2}[\phi(f,\tau) + \phi^*(f,-\tau)] \qquad (30)$$

   and

$$\mathcal{P}_{C8}\phi(f,\tau) = \frac{1}{2}[\phi(f,\tau) + \phi^*(-f,\tau)]. \qquad (31)$$

3. **Relaxed Interference Projection.**

   Motivated by Equation 8, the projection operator corresponding to the relaxed interference term in Constraint 3 corresponding to Equation 9 is

$$\mathcal{P}_{C3}\Phi(f,u) = \Phi(f,u)\Pi(\frac{f}{2\Delta}) \qquad (32)$$

   Note that if $\Delta$ is large enough and $B$ is small enough, the frequency resolution projection in Equation 27 subsumes this projection.

4. **Power Spectral Density Marginal / Non-Negative / Cone Constraint.**

   In some cases, projections can be best described on the intersection of two or more convex constraints. Combining the time resolution constraint (1), the non-negativity constraint (9) and the power spectral density constraint (4) in Equation 12, we can write the projection on the intersection of the three sets as the convex set operator

$$\mathcal{P}_{C_1 \cap C_4 \cap C_9} \hat{\phi}(t,\tau) = [\hat{\phi}(t,\tau) + \varphi(\tau)]\Pi(\frac{t}{\tau}) \qquad (33)$$

   where $\cap$ denotes intersection and

$$\varphi(\tau) = \frac{1}{|\tau|}[1 - \int_{t=-\frac{\tau}{2}}^{\frac{\tau}{2}} \hat{\phi}(t,\tau)dt] \qquad (34)$$

## 3.3 Alternating Projections

There are three fundamental lemmas in the theory of POCS. We will state each lemma and illustrate it geometrically.

*Lemma* 1. **Alternately projecting between two or more convex sets with a nonempty intersection will iteratively converge to a point common to all sets** [18, 16]. This is illustrated in Figure 4. Note that the point of convergence generally depends on the initialization. If, however, there is a single point of intersection (*e.g.* two lines), then convergence will be independent of the initialization.

*Lemma* 2. **Alternately projecting between two nonintersecting convex sets will converge to a limit cycle between points in each set closest to the other set** [10]. This is illustrated in Figure 5. This property can be used to find the best member in a set that is closest to another set in the mean square sense. Note that, as can be visualized in the case of two parallel line convex sets, the limit cycle is not unique.

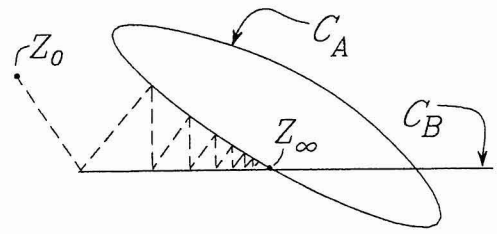


Figure 4: Alternating projection between two intersecting convex sets, $C_A$ and $C_B$, iteratively approaches a fixed point, $Z_\infty$, common to both sets. If there is more that one point in the intersection, the fixed point will be a function of the initialization of the interation which, in this example, is $Z_0$.

This property generalizes to more than three sets in the following sense. Let two or more constraints have a nonempty intersection, $C_a$. Let two or more other constraints have a nonempty intersection, $C_b$. If $C_a$ and $C_b$ do not intersect, then POCS will converge to a limit cycle between points convex sets $C_a$ and $C_b$ each closest to the other in the mean square sense.

*Lemma* 3. **Alternately projecting between three or more nonintersecting convex sets will result in a limit cycle that can be de-**

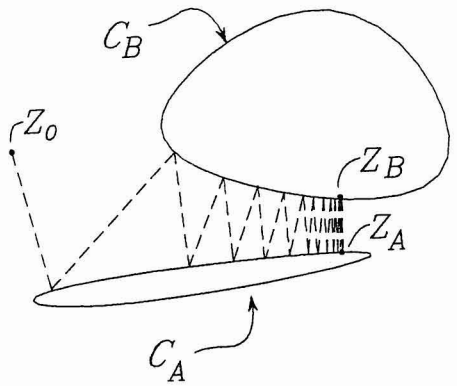


Figure 5: Alternating projection between two nonintersecting convex sets, $C_A$ and $C_B$ iteratively approaches a limit cycle between two points in each set. In this illustration, these points are $Z_A$ and $Z_B$. Note that $Z_A$ is the point in $C_A$ that is closest to $C_B$ and *visa versa*. The solution is thus a minimum mean square error solution. Although not always the case, the limit cycle here is independent of initialization, $Z_0$. If there exists more than one possible limit cycle, each will have points separated by the same distance.

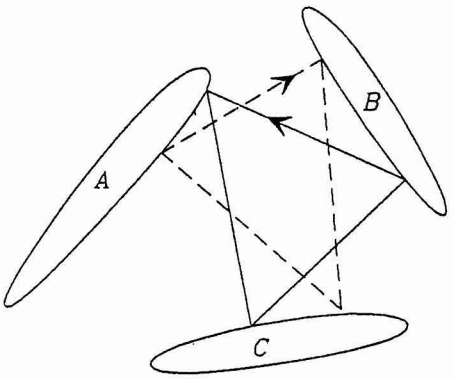


Figure 6: A number of different limit cycles can exist when three or more convex sets do not intersect. Here, projecting from set $A$ to $B$ to $C$ gives a different limit cycle than projecting them in reverse order.

**pendent on both the ordering of the projections and the initialization** [19]. This final lemma states, unfortunately, that POCS can yield results of questionable worth when three or more of the convex sets do not intersect. Two different limit cycles corresponding to different orderings of the projection are geometrically illustrated in Figure 6 for the case of three nonintersecting sets.

# 4 POCS Kernel Synthesis

The use of POCS in the design of GTFR kernels is now evident. We choose from a menu of convex constraints that we desire our GTFR to obey. By alternately projecting between the corresponding convex sets, we hope to synthesize a corresponding kernel. If the convex sets meet the suppositions of Lemma 1, a kernel

meeting all constraints will be generated. If the constraints in Lemma 2 are met, we will be guaranteed that the constraints have been met in a mean square sense. This may or may not be acceptable depending on the magnitude of the mean square error. Note, however, that this is a problem of the problem rather than that of the synthesis method. In other words, the distances between the constraint sets are too large to allow for any acceptable solution.

To illustrate the potential use of POCS in kernel design, we present two preliminary examples. Both examples were computed on a 128 x 128 grid. The kernels in both examples used both the cone and bow tie constraints. The value of $T$ in each case corresponded to truncating the grid so that the cone was a peak to peak height of 64. The value of $2B$ was chosen to be five intervals. Since $B$ was chosen to be small, there was no need to specify a value for $\Delta$ for the interference suppression constraint. Both examples resulted in a kernel that was positive and symmetric.

**Example 1** used, in addition, both marginal constraints. The resulting kernel is pictured in Figure 7. It resembles a $t$-truncated Born-Jordon kernel which has a $\frac{1}{|\tau|}$ taper within the cone. Indeed, for $B = \infty$ and $T = \infty$, the Born-Jordon kernel satisfies all the constraints. Specifically,

$$\hat{\phi}(t;\tau) = \frac{1}{|\tau|}\Pi(\frac{t}{\tau}) \qquad (35)$$

satisfies the cone constraint in Equation 5. Furthermore, the marginal constraints in Equations 15 and 18 are met as are the symmetry constraints of Equations 19, 21 and 23, the realness constraint of Equation 20 and the nonegativity constraint in Equation 25. Furthermore,

$$\Phi(f;u) = \frac{1}{|f|}\Pi(\frac{u}{f}) \qquad (36)$$

satisfies the untruncated bow tie constraint.

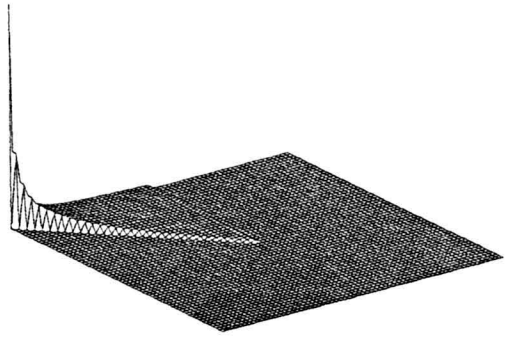

Figure 7: One quadrant of the symmetric cone kernel on the $(t,\tau)$ plane synthesized using all the POCS constraints listed in this paper. The iteration reached a limit cycle. Thus, all of the constraints could not be simultaneously met for finite $T$ and $B$.

Historically, this POCS result first prompted the authors to investigate cone kernels with uniform taper [3, 20].

Application of the kernel in Figure 7 to two converging linear chirps [9, 13] resulted in the dB waterfall display in Figure 8. From floor to peak is 25dB.

**Example 2** removed the marginal constraints in the kernel design and resulted in the kernel in Figure 9. The outcome of the POCS

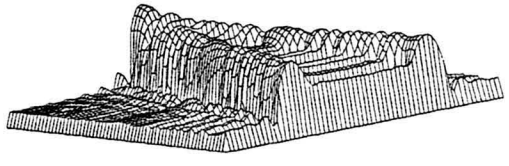

Figure 8: Waterfall display of two linearly converging chirps using the POCS designed kernel in the previous figure. There is significant smoothing between the tones.

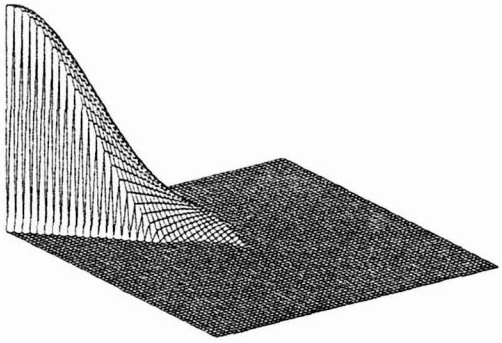

Figure 9: One quadrant of the symmetric cone kernel on the $(t, \tau)$ plane synthesized using all the POCS constraints listed in this paper except the power spectral density and instantaneous power marginals.

design, smoothed with a Hanning window, was applied to the same linear chirp problem. The result is shown in Figure 10 using a 35dB floor to peak range. Compare this with a cone shaped kernel result in Figure 11 with uniform Hanning window taper in the $\tau$ direction. The same 35dB range is used. For this example, the POCS kernel seems to perform better in terms of frequency resolution and interference suppression. To complete the comparison, similarly scaled plots of the spectrogram and Wigner distribution for the same signal are shown respectively in Figure 12 and 13.

## 5 Conclusions

We have presented a technique whereby kernels for use in Cohen's class of GTFR's can be synthesized in accordance to desired properties using the method of *projection onto convex sets*. The ultimate success of this synthesis methodology is dependant on the performance of these kernels in generating GTFR's of signals in specific applications.

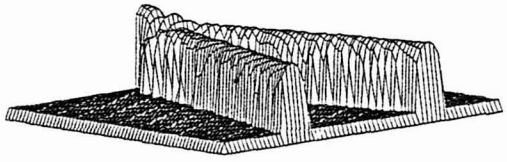

Figure 10: Waterfall display of two linearly converging chirps using the POCS designed kernel in the previous figure. The result is quite good.

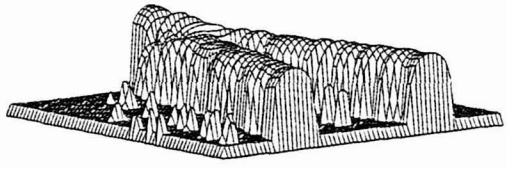

Figure 11: Use of a cone shaped kernel with uniform Hanning taper in the $\tau$ direction on the two chirp signal. The 35dB range is the same as in the previous figure.

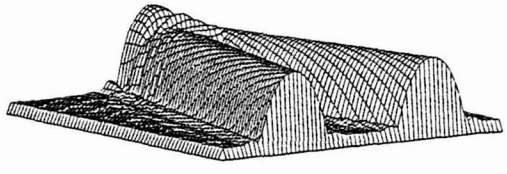

Figure 12: Spectrogram of the two chirp signal.

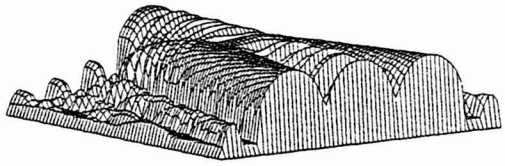

Figure 13: Wigner distribution of the two chirp signal.

## 6 Acknowledgements

The authors express their appreciation to Hal Philipp of *Philipp Technologies Corporation*, Pat Loughlin of the *Interactive Systems Design Lab* and Loren Laybourn of *Raytron* for their input and encouragement.

## References

[1] L.E. Atlas, P. Loughlin, J. Pitton & W. Fox, "Applications of cone-shaped kernel time-frequency representations to speech and sonar analysis", *Proc. Int. Sym. on Sig. Proc. & Appl.*, Gold Coast, Australia, 27-31 August 1990.

[2] L.E. Atlas, W. Kooiman, P. Loughlin & Ron Cole, "New nonstationary techniques for the analysis and display of speech transients", *Proceedings of the IEEE International Conference on Acoustics, Speech and Signal Processing*, Albuquerque, New Mexico, p.3885, 1990.

[3] L.E. Atlas, Y. Zhao and R.J. Marks II, "Application of the generalized time-frequency representation to speech signal analysis", *Proceedings of the IEEE Pacific Rim Conference on Communications, Computers and Signal Processing*, pp.517-519, Victoria, B.C. Canada, June 4-5, 1987.

[4] M.R. Civanlar & H.J. Trussel, "Digital signal restoration using fuzzy sets", *IEEE Transactions on Acoustics, Speech and Signal Processing*, vol. ASSP-34, p.919 (1986).

[5] L. Cohen, "Generalized phase-space distribution functions" *J. Math. Physics*, vol.7, pp.781-786 (1966).

[6] L. Cohen, "Time-frequency distributions - a review", *Proceedings of the IEEE*, vol.77, pp.941-981 (1989).

[7] T.A.C.M. Claasen and W.F.G. Mecklenbrauker, "The Wigner distribution, a tool for time-frequency signal analysis, Part 2: discrete time signals", *Philips J. Res.*, vol.35, pp.277-300, 1980.

[8] T.A.C.M. Claasen and W.F.G. Mecklenbrauker, "The Wigner distribution, a tool for time-frequency signal analysis, Part 3: relations with other time-frequency signal transformations", *Philips J. Res.*, vol.35, pp.373-389, 1980.

[9] H.Choi & W. Williams, "Improved time-frequency representation of multicomponent signals using exponential kernels", *IEEE Trans. Acoust., Speech, and Sig. Proc.*, vol.37, pp.862-871, 1989.

[10] M.H. Goldburg and R.J. Marks II "Signal synthesis in the presence of an inconsistent set of constraints", *IEEE Transactions on Circuits and Systems*, vol. CAS-32 pp. 647-663 (1985).

[11] R.J. Marks II, "A class of continuous level associative memory neural nets", *Applied Optics*, vol. 26, pp.2005-2009 (1987).

[12] R.J. Marks II, S. Oh and L.E. Atlas, "Alternating projection neural networks", *IEEE Transactions on Circuits and Systems*, vol.36, pp.846-857 (1989).

[13] S.Oh and R.J. Marks II, "Some properties of the generalized time frequency representation with cone shaped kernel", submitted for publication to *IEEE Transactions on Acoustics, Speech and Signal Processing.*

[14] S.Oh and R.J. Marks II, "Tone interference in Cohen's Generalized Time-Frequency Representation", ISDR Report 90-7A, Department of Electrical Engineering, University of Washington (June, 1990).

[15] M.I. Sezan and H. Stark, "Image restoration by method of convex set projections: Part II - Applications and Numerical Results", *IEEE Trans. Med. Imaging*, vol MI-1, pp.95-101, 1982.

[16] H. Stark, editor, **Image Recovery: Theory and Application**, (Academic Press, Orlando, 1987).

[17] S.J. Yen & H. Stark, "Iterative and one-step reconstruction from nonuniform samples by convex projections", *Journal of the Optical Society of America-A*, vol.7, pp.491-499 (1990).

[18] D.C. Youla and H. Webb, "Image restoration by method of convex set projections: Part I - Theory", *IEEE Trans. Med. Imaging*, vol MI-1, pp.81-94, 1982.

[19] D.C. Youla and V. Velasco, "Extensions of a result on the synthesis of signals in the presence of inconsistent constraints", *IEEE Transactions on Circuits and Systems*, vol. CAS-33, pp.465-468 (1986).

[20] Y. Zhao, L.E. Atlas and R.J. Marks II, "The use of cone-shape kernels for generalized time-frequency representations of nonstationary signals", *IEEE Transactions on Acoustics, Speech and Signal Processing*, vol. 38, pp.1084-1091 (1990).